Available online at www.sciencedirect.com
SCIENCE DIRECT®
Bioorganic & Medicinal Chemistry Letters 14 (2004) 3165–3168
Bioorganic & Medicinal Chemistry Letters

Structure-based design, synthesis, and antimicrobial activity of purine derived SAH/MTA nucleosidase inhibitors

Martina E. Tedder,[a] Zhe Nie,[a] Stephen Margosiak,[b] Shaosong Chu,[a] Victoria A. Feher,[c] Robert Almassy,[c] Krzysztof Appelt[a] and Kraig M. Yager[a,*]

[a]*Department of Medicinal Chemistry, Quorex Pharmaceuticals, Carlsbad, CA 92008, USA*
[b]*Department of Protein Chemistry, Quorex Pharmaceuticals, Carlsbad, CA 92008, USA*
[c]*Department of Structural Biology, Quorex Pharmaceuticals, Carlsbad, CA 92008, USA*

Received 12 March 2004; revised 2 April 2004; accepted 3 April 2004

Abstract—The structure-based design, synthesis, and biological activity of novel inhibitors of S-adenosyl homocysteine/methylthioadenosine (SAH/MTA) nucleosidase are described. Using 6-substituted purine and deaza purines as the core scaffolds, a systematic and structure guided series of modifications provided low nM inhibitors with broad-spectrum antimicrobial activity.

Multiple drug resistant (MDR) pathogenic bacteria present a major obstacle to the effective treatment of serious hospital and community-based infections. Emergence of resistant organisms continues unabated and, along with an overall increase in the number of infections worldwide, drives the need for new agents effective against them.[1] Ideally such antibacterial agents will hit essential proteins that (1) appear in as many bacterial pathogens as possible but (2) differ significantly from related mammalian proteins, to yield a broad spectrum of activity with minimal mechanism-based toxicity. We describe here the rationale and results of this approach.

S-adenosyl homocysteine/methylthioadenosine (SAH/MTA) nucleosidase, hereafter MTA nucleosidase, has been shown to be essential in a representative number of pathogenic bacteria.[2] In addition, bioinformatics analyses reveal a MTA nucleosidase active site pocket that is highly conserved across bacterial species and contains regions distinct from related mammalian proteins, namely, methylthioadenosine phosphorylase, and purine nucleotide phosphorylase.[3,4] These features provide an enzyme target well suited for a structure-based drug design approach toward development of a broad-spectrum antibiotic with low potential for mechanism-based toxicity in humans.[5] MTA nucleosidase is a product of the highly conserved *pfs* gene (Fig. 1).[6] Functionally, inhibition of MTA nucleosidase activity eliminates the downstream synthesis of the quorum sensing autoinducer AI-2.[7] Loss of AI-2 is expected to attenuate quorum sensing and expression of pathogenic virulence factors. Additionally, the accumulation of the toxic SAH and MTA nucleosidase substrates elicits inhibition of various essential methyltransferase reactions and affects the recycling of the adenine and methionine necessary for DNA and protein synthesis, respectively.

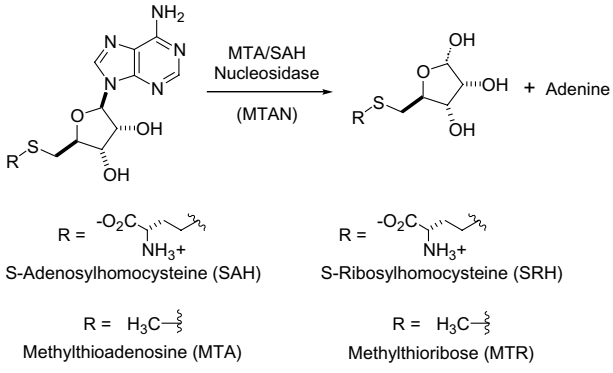

Figure 1. Reaction catalyzed by MTA nucleosidase in vivo.

Keywords: Structure-based drug design; Antimicrobial.
* Corresponding author. Tel.: +1-760-494-6230; fax: +1-760-602-1915; e-mail: kyager@quorex.com

0960-894X/$ - see front matter © 2004 Elsevier Ltd. All rights reserved.
doi:10.1016/j.bmcl.2004.04.006

Selection of compounds for screening in the MTA nucleosidase activity assay[8] was accomplished by filtering a virtual library of ~400,000 commercially available compounds to approximately 1300 satisfying the following criteria; (1) all compounds were to possess three pharmacophoric features identified from inspection of homology model: substrate complexes, (2) all compounds had molecular volumes not exceeding that of the homology model and (3) all compounds met Lipinski property guidelines (i.e., molecular weight < 500, $-2.0 < C\log P < 5.0$).[9] The resulting data set was clustered by 2D fingerprint diversity and a representative selection made using SELECTOR (Tripos, Inc.). Purine-containing compounds were naturally included in the selection because of their similarity to the substrate and high population in commercially available compound libraries.

Co-crystallization and X-ray structural determination with potent inhibitors and *E. coli* MTA nucleosidase and other pathogenic *pfs* proteins revealed the mode of inhibitor binding within the active site. These co-structures provided the structural information by which key individual compounds and focused libraries were designed. Exploiting this iterative process, we were able to identify potent inhibitors of MTA nucleosidase in only a few cycles.

Our initial lead in this series was the benzylamine derivative **2a** ($K_i = 1\,\mu M$). The co-structure of **2a** with MTA nucleosidase revealed an unexpected mode of binding. The purine core does not bind similarly to the adenine analogs of the three co-crystal structures published; adenine·MTA nucleosidase, MTT·MTA nucleosidase and FMA·MTA nucleosidase,[6e,f] (Fig. 2). Instead, it adopts a bound conformation where the purine N3 and N9 nitrogens establish hydrogen bonds with the protein backbone residue I152 (Fig. 2b). In addition, the C6 NH forms water-mediated hydrogen bonds with S76 and S196. Additional affinity is realized from π–π stacking with F151 and hydrophobic interactions with the 4-carboxyphenyl substituent. A conformational change in the region of D197 is also observed. This residue rotates away from the ligand, further expanding the 'open' pocket volume relative to that observed in the adenine·MTA nucleosidase complex and alters the hydrogen-bonding pattern between D197 and S196.

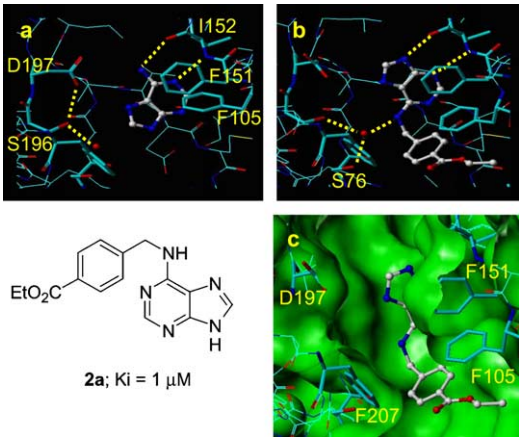

Figure 2. Screening hit **2a** co-crystallized with MTA nucleosidase (b) in a different binding mode than predicted by analogy to the adenine·MTA nucleosidase co-crystal structure (a). Isoleucine 152 and phenylalanine 151 are involved in key binding interactions with the inhibitor. (c) The solvent accessible surface (green) is included in the active site to illustrate the burial of **2a** by phenylalanine residues 151, 105, and 207 and the expanded pocket at the top of the binding site.

In terms of medicinal chemistry, the first goal was to find a suitable replacement for the ester substituent of the benzyl moiety. From the crystal co-structure, there appeared to be significant additional interactions to be gained in this region of the active site. Synthetically, this was a straightforward operation were nucleophilic displacement of the purine 6-chloro group by amines provided **2a**–**j** in good yield (Scheme 1).[10]

Because this area opens up to solvent, solubilizing groups at this site were explored in efforts to improve ligand physiochemical properties (Table 1).

Additionally, the adenine-like core was optimized to move away from the known toxicity associated with purine scaffolds. The co-crystal structure implies the 9 and 3 positions of the heterocycle require a H-donor and H-acceptor, respectively. With these criteria, each of the other ring nitrogens was systematically replaced with aromatic CH groups (Scheme 2, Table 2). Ultimately it was determined that, in addition to the purine scaffold of **2a** and homologs, the imidazo pyridines[11] **6**–**8** and pyrrolo-pyrimidines **10** and **11** represented active scaffolds for further SAR studies.

Scheme 3 illustrates compounds designed to assess the effects on potency of a cyclopentylethyl substituent at 'C8' on the purine (cf. **17** and **16**) and azabenzimidazole (e.g., **8**) scaffolds. As predicted by modeling, the increase in affinity was profound with **17** being ca. 180-fold more active than the 'C8' unsubstituted derivative **2j**. The effects on potency are less pronounced in the 4-carbomethoxybenzyl series, specifically **16** is roughly 35-fold more active than **2a** and only 18-fold more active than the C8 ethyl derivative **15**. Potency of the imidazo pyridine scaffold is also enhanced, that is **8**, however the improved interactions realized with the optimized pendent groups is not sufficient to mitigate the loss in affinity due, most likely, to the poor H-bond accepting capacity of the 4-aminopyridine ring system (Table 3).

The co-crystal structure for **17**·MTA nucleosidase complex was elucidated to 2.1 Å (Fig. 3). The cyclopentylethyl group creates a number of strong hydrophobic interactions while the H-bonding network

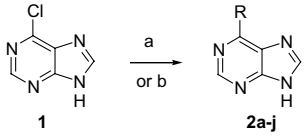

Scheme 1. (a) RNH_2, $^iPr_2NEt$, ^{n}BuOH, reflux. (b) ROH, ^{t}BuOK, THF.

Table 1. Inhibition data for C6-substituted purines

2	R	K_i (μM)
a	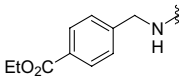	1
b	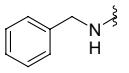	90
c	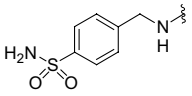	20.0
d	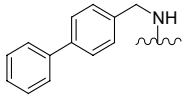	1.0
e	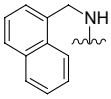	64
f	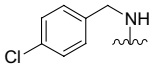	33
g	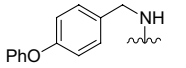	1.6
h	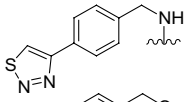	5.0
i	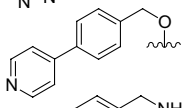	1.5
j	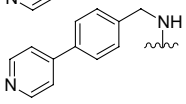	0.5

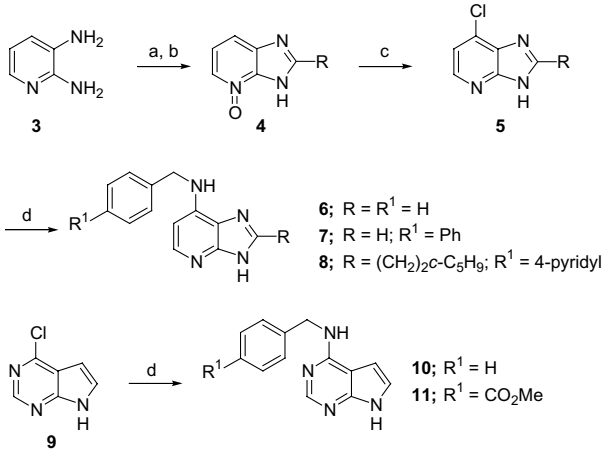

Scheme 2. (a) R = H; $(EtO)_3CH$, $EtSO_3H$, 100 °C. R = $(CH_2)_2$-*c*-C_5H_9; *c*-$C_5H_9(CH_2)_2COCl$, $^iPr_2NEt$, $CHCl_3$, then AcOH, $EtSO_3H$, reflux; (b) 30% H_2O_2, AcOH, 50 °C; (c) $POCl_3$, 110 °C; (d) $R^1C_6H_4CH_2NH_2$ (3 equiv), ^{n}BuOH, reflux.

between the purine ring and protein backbone is much like that observed in the **2a**·MTA nucleosidase complex. It was noted that the 4-pyridylphenyl adopts a nearly planar conformation. The measured torsion angle between atoms a–d (Fig. 3) is 8° for the molecule in one monomer and 16° in the other monomer of the dimer.[12]

Table 2. Activities of alternate heterocyclic cores

Compound	K_i (μM)
6	50
7	170
8	0.306
10	72
11	2.2

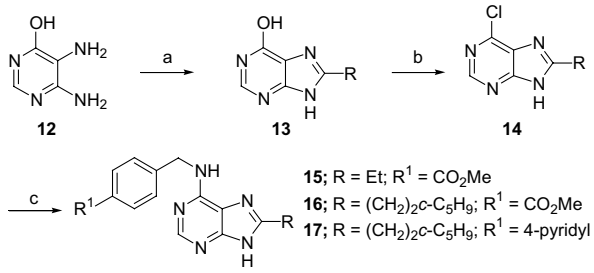

Scheme 3. (a) R = Et; $(EtO)_3CEt$, $EtSO_3H$, 100 °C, then 10% aq HCl. R = $(CH_2)_2$-*c*-C_5H_9; *c*-$C_5H_9(CH_2)_2COCl$, $^iPr_2NEt$, $CHCl_3$, then 4N NaOH, EtOH, reflux; (b) $POCl_3$, 110 °C; (c) $R^1C_6H_4CH_2NH_2$, $^iPr_2NEt$, ^{n}BuOH, reflux.

Table 3. Inhibitory activity of C2 substituted purine derivatives

Compound	K_i (μM)
15	0.79
16	0.043
17	0.0028

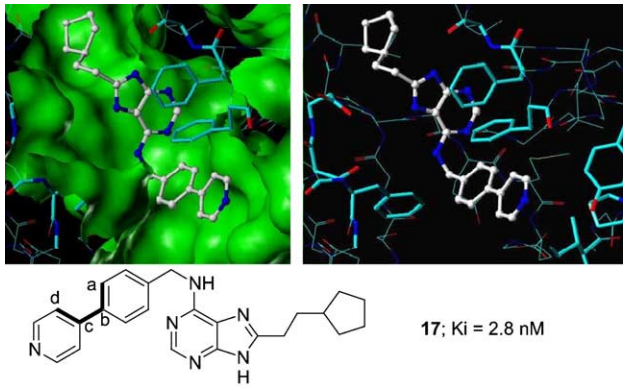

Figure 3. Compound **17** bound to the MTA nucleosidase active site as determined by X-ray crystallography analysis.

It is well known that deviation from the preferred biphenyl 45° torsion (in gas phase) constitutes an upper limit of ~3 kcal/mol in unfavorable steric interactions. However, this is often overridden by ring preference for ring stacking in small molecule crystal structures. To determine whether a significant (⩾10-fold) increase in affinity would be realized should it be possible to regain the system binding energy lost to these unfavorable bond angle geometries, the 4-pyridylpyrimidine derivative **23**, was targeted for synthesis. The pyrimidinyl nitrogens *a* and *a*′ (2-fold degeneracy) present no hindrance to establishment of an essentially coplanar orientation of the two aromatic rings. Additionally, by incorporation of a pyrimidine into the side chain it should be possible to

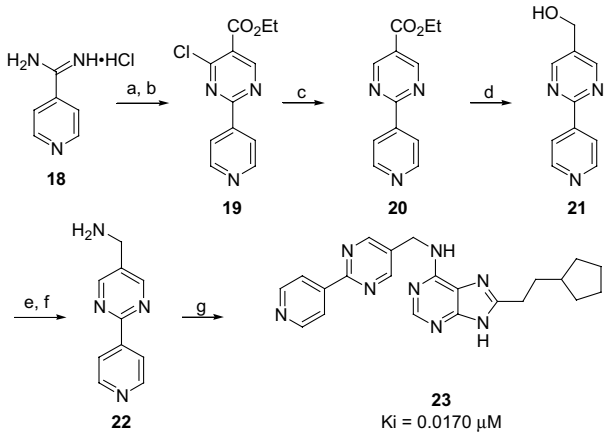

Scheme 4. (a) Diethyl ethoxymethylenemalonate, KOEt, EtOH, reflux; (b) $SOCl_2$, cat. DMF, reflux; (c) H_2, 20% $Pd(OH)_2/C$, $^iPr_2NEt$, EtOH; (d) DIBAL-H, toluene, THF; (e) PPh_3, NaN_3, CCl_4, DMF; (f) H_2, 20% $Pd(OH)_2/C$, MeOH; (g) **14**; $R = (CH_2)_2c\text{-}C_5H_9$, $^iPr_2NEt$, ^{n}BuOH, 95 °C.

maintain a charge- and dipole-neutral proximal ring system. Inhibitor **23** was prepared according to Scheme 4. Thus condensation of 4-amidinopyridine (**18**) with diethyl ethoxymethylenemalonate provided an intermediate hydroxy pyrimidine that was converted directly to chloro ester **19**.[13] Sequential reductions provided benzyl alcohol derivative **21**.

Rather than a gain in affinity, a 6-fold drop in apparent K_i was observed. There are at least two plausible, and not necessarily mutually exclusive explanations for this result. One is that the acute dihedral angle is an artifact of protein crystal packing forces. Another is that the recovered system energy is outweighed by energetic penalties associated with desolvation of the inhibitor upon binding.

A series of purine and deaza purine-based inhibitors of MTA nucleosidase has been developed. Structure-based modification of lead structure **2a**, led to the discovery of **16** and **17**, low molecular weight inhibitors with nanomolar potency in an enzyme inhibition assay. These compounds were also active in antimicrobial assays, inhibiting the growth of three important pathogenic genera.[14]

Acknowledgements

The authors thank Drs. Carol Dammel and James Levin of our Preclinical Microbiology Department for MIC determinations and fruitful discussions.

References and notes

1. Projan, S. J. *Current Opinion Pharmacol.* **2002**, *2*, 513–522.
2. Viable *pfs*-null mutants of *Haemophilus influenzae*, *Streptococcus pneumoniae*, and *Staphylococcus aureus* could not be generated. The *pfs* gene is not essential in *Enterococcus faecalis* and may therefore not be essential in other Gram-positive strains where efflux pumps may be upregulated. Grant, C. and Levin, J., Quorex Pharmaceuticals, unpublished results.
3. Mao, C.; Cook, W. J.; Zhou, M.; Federov, A. A.; Almo, S. C.; Ealick, S. E. *Biochemistry* **1998**, *37*, 7135–7146.
4. Koellner, G.; Luic, M.; Shugar, D.; Saenger, W.; Bzowska, A. *J. Mol. Biol.* **1998**, *280*, 153–166.
5. Li, X.; Chu, S.; Feher, V. A.; Khalili, M.; Nie, Z.; Margosiak, S.; Nikulin, V.; Sprankle, K. G.; Tedder, M. E.; Almassy, R.; Levin, J.; Appelt, K.; Yager, K. M. *J. Med. Chem.* **2003**, *46*, 5663–5673.
6. (a) Della Ragione, F.; Porcelli, M.; Carteni-Farina, M.; Zappia, V.; Pegg, A. E. *Biochem. J.* **1985**, *232*, 335–341; (b) Cornell, K. A.; Swarts, W. E.; Barry, R. D.; Riscoe, M. K. *Biochem. Biophys. Res. Comm.* **1996**, *228*, 724–732; (c) Allart, B.; Gatel, M.; Guillerm, D.; Guillerm, G. *Eur. J. Biochem.* **1998**, *256*, 155–162; (d) Cornell, K. A.; Riscoe, M. K. *Biochim. Biophys. Acta* **1998**, *1396*, 8–14; (e) Lee, J. E.; Cornell, K. A.; Riscoe, M. K.; Howell, P. L. *Structure* **2001**, *9*, 941–953; (f) Lee, J. E.; Corrnell, K. A.; Riscoe, M. K.; Howell, P. L. *J. Biol. Chem.* **2003**, *278*, 8761–8770.
7. (a) Surette, M. G.; Miller, M. B.; Bassler, B. L. *Proc. Natl. Acad. Sci. U.S.A.* **1999**, *96*, 1639–1644; (b) Schauder, S.; Shokat, K.; Surette, M. G.; Bassler, B. L. *Mol. Biol.* **2001**, *41*, 463–476.
8. Details of the enzymatic assays used in this study may be found in Ref. 5.
9. (a) Lipinski, C. A.; Lombardo, F.; Dominy, B. W.; Feeney, P. F. *Adv. Drug Delivery Rev.* **1997**, 23; (b) Unity and Selector software Tripos, Inc. St. Louis, MO; (c) Sheridan, R. P.; Nachbar, R. B.; Bush, B. L. *J. Comp-Aided Mol. Des.* **1994**, *8*, 323–340.
10. (a) Seyama, F.; Akahori, K.; Sakata, Y.; Misumi, S.; Aida, M.; Nagata, C. *J. Am. Chem. Soc.* **1988**, *110*, 2192–2201; (b) Jacobsen, K. A.; Siddiqi, S. M.; Olah, M. E.; Ji, X.-D.; Melman, N.; Bellamkonda, K.; Meshulam, Y.; Stiles, G. L.; Kim, H. O. *J. Med. Chem.* **1995**, *38*, 1720–1735; (c) Baker, B. F.; Dervan, P. B. *J. Am. Chem. Soc.* **1989**, *111*, 2700–2712; (d) Shadid, B.; van der Plas, H. C.; Boesten, W. H. J.; Kamphuis, J.; Meijer, E. M.; Schoemaker, H. E. *Tetrahedron* **1990**, *46*, 913–920.
11. Itoh, T.; Ono, K.; Sugawara, T.; Mizuno, Y. *J. Heterocycl. Chem.* **1982**, *19*, 513–517.
12. MTA nucleosidase crystallizes with two molecules per asymmetric unit. Periodically, small differences in side-chain and inhibitor conformations were observed between subunits.
13. Palanki, M. S.; Erdman, P. E.; Manning, A. M.; Ow, A.; Ransone, L. J.; Spooner, C.; Suto, C.; Suto, M. *Bioorg. Med. Chem. Lett.* **2000**, *10*, 1645–1648.
14. Minimum inhibitory concentration (MIC) values were typically $\geqslant 30\,\mu M$ ($\sim 12\,\mu g/mL$).